https://doi.org/10.20965/jrm.2007.p0013

Paper:

Development of a Quadruped Walking Robot TITAN XI for Steep Slope Operation

– Step Over Gait to Avoid Concrete Frames on Steep Slopes –

Ryuichi Hodoshima*, Takahiro Doi, Yasushi Fukuda***, Shigeo Hirose*, Toshihito Okamoto****, and Junichi Mori****

*Mechanical and Aerospace Engineering of Science and Engineering, Tokyo Institute of Technology
2-12-1 Ookayama, Meguro-ku, Tokyo 152-8552, Japan
E-mail: hodoshima@robotics.mes.titech.ac.jp
**Life System Science and Technology, Chukyo University
101 Tokodachi, Kaizu-cho, Toyota-shi, Aichi 470-0393, Japan
***Mechanical System of Engineering, Tamagawa University
6-1-1 Tamagawagakuen, Machida-shi, Tokyo 194-8610, Japan
****TAISHO KENSETU Corporation
2695 Kaneda, Chosei-mura, Chosei-gun, Chiba 299-4332, Japan
[Received September 26, 2005; accepted July 14, 2006]

We detail a step over gait for a quadruped walking robot that maintains a continuous walking with sufficient stability margin for avoiding ferroconcrete reinforcement frames covering steep slopes. For this gait, the robot must adapt itself to terrain and step over these frames. We propose a terrain-adaptive gait based on an intermittent crawl gait using map information. After introducing the gait control algorithm, we show results of graphical simulation to verify the proposed algorithm. Then, these discussions are established by walking experiments using the developed quadruped walking robot named TITAN XI.

Keywords: quadruped walking robot, intermittent crawl gait, terrain-adaptive gait, concrete frame avoidance, map generation

1. Introduction

The legged robots contact the ground with discrete points and the contact points can be arbitrary selected according terrain conditions. Therefore, these robots are suitable for uneven terrain locomotion. These robots also can control their pose freely on uneven terrain within some limited range by driving supporting legs such as a parallel-link arm at standstill. It can be utilized not only for motion, but also for rest.

Focusing on these features, we are developing a quadruped walking robot [1] for practical operation on slopes to automate part of slope reinforcement in which workers must negotiate steep and often dangerous slopes. The most practical maneuvering for construction robots is basically done by users, since autonomous motion still involves many problems and the working environment is complex. Working robots have multiple degrees of freedom, making it difficult for an operator to directly control all actuators. For the operator to maneuver a walking robot, they must be able to control robot motion by simple commands such as instructions for walking paths. The environment these robots operate in is steep slopes covered with deformed ferroconcrete grids (**Fig. 1**). Walking robots must step over these grids to avoid damaging themselves. Such complex environments are difficult to negotiate using a regular gait consisting of simple repetitive leg motions, so what is needed are non-regular gait (adaptive gait) that adapt leg motion based on terrain conditions.

Fig. 1. Steep slope covered with concrete frames.

We systematically studied the terrain-adaptive gait for a quadruped walking robot that walks basically on plain ground [2]. Robots operating on slopes require maximized static stability, easy operation, and it is indispensable to define a special terrain-adaptive gait for these robots. We propose gait control that generates a gait enabling a large quadruped walking robot to step over ferroconcrete frames with sufficient stability based on map

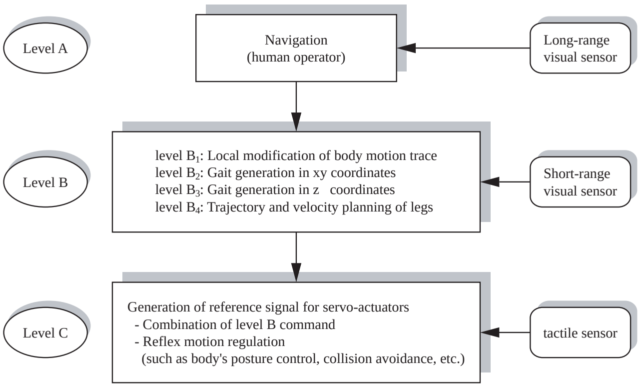

Fig. 2. Hierarchical control system of a walking vehicle [2].

information under the slope conditions above. Section 2 presents control configuration for walking and postulates of the gait. Section 3 specifies problems, Section 4 introduces basic concepts, Sections 5 and 6 detail gait generation, Section 7 confirms the feasibility of our proposal through simulation, and Section 8 verifies effectiveness by prototyping TITAN XI in walking experiments. Section 9 presents conclusions.

2. Control System Configuration

We reported [2] that walking robot control are preferably classified into 3 control levels (**Fig. 2**). Level A involves navigation, strategic motion generated, for example, based human command. Level B involves gait control, which is further divided into (1) local center of gravity (COG) trajectory modification, (2) planar gait generation, (3) height gait generation, and (4) leg trajectory and speed planning. Level C involves reflex motion adjustment, which generates emergency motion while executing instructions. We use this control and Level B, detailed below.

3. Problem Setting for Gait Control

We use the following symbols:

$f, \bar{f}, r, \bar{r}$: f for the front leg and r for the rear leg on the same side to a leg, and $\bar{f}$ and $\bar{r}$ for the opposite side.

i: indication to designate a leg ($i = 1, \ldots, 4$) or ($i = f, \bar{f}, r, \bar{r}$)

k: cycle number after walking start

u: indication for a swing leg

g: indication for COG

$\Sigma_w(O_w\text{-}x_w y_w z_w)$: absolute (world) coordinates

$\Sigma_b(O_b\text{-}x_b y_b z_b)$: body coordinates

L_G: planar projection line of a walking path

S_{NE}: normalized energy (NE) stability margin

S_{NE}^c: critical normalized energy stability margin

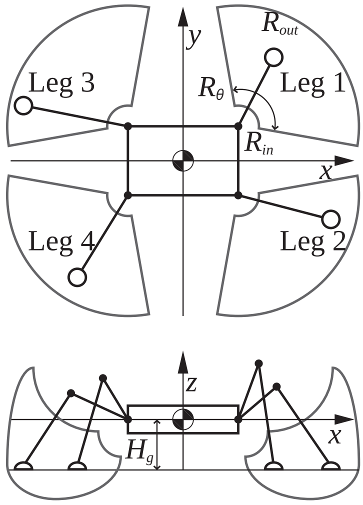

Fig. 3. The dimensions of reachable area for a quadruped walking robot.

R_{out}: outer radius for an area reachable by a leg

R_{in}: inner radius for an area reachable by a leg

R_θ: leg rotation angle range

C_k: "k"th walking cycle

H_g: height of COG to be ensured

A_i: area reachable by leg i

D_u: foothold search area for swing leg u

$\boldsymbol{P}_a(P_{ax}, P_{ay}, P_{az})$: position indicated by "a"

$\boldsymbol{J}_u(J_{ux}, J_{uy}, J_{uz})$: foothold position for swing leg u

$\boldsymbol{I}_u(I_{ux}, I_{uy}, I_{uz})$: initial foothold-search position for determining $\boldsymbol{J}_u$

$\boldsymbol{G}, \bar{\boldsymbol{G}}$: COG shift vector indicating the first and next COG shift.

$\boldsymbol{L}, \bar{\boldsymbol{L}}$: COG longitudinal vectors corresponding to each COG vector parallel to L_G

$\boldsymbol{W}, \bar{\boldsymbol{W}}$: COG lateral vectors corresponding to each COG vector left and right orthogonal to L_G

$\boldsymbol{l}_i(l_{ix}, l_{iy}, l_{iz})$: vector for COG to proceed along a walking path L_G by grounding leg i. A norm of this vector is the distance brought by leg i motion in the opposite direction of L_G on Σ_b and restricted by area reachable by a leg.

$\boldsymbol{g}_i(g_{ix}, g_{iy}, g_{iz})$: COG shift vector generated by supporting leg i.

$\boldsymbol{L}_{std}, \bar{\boldsymbol{L}}_{std}, \boldsymbol{W}_{std}, \bar{\boldsymbol{W}}_{std}$: standard intermittent crawl gait parameters. COG longitudinal vectors and COG lateral vectors corresponding to each COG shift (**Fig. 7**).

We discuss issues for a slope-operation quadruped TITAN XI, we are developing. Due to rotation around a pivot, TITAN XI leg motion is fan-shaped (**Fig. 3**). Gen-

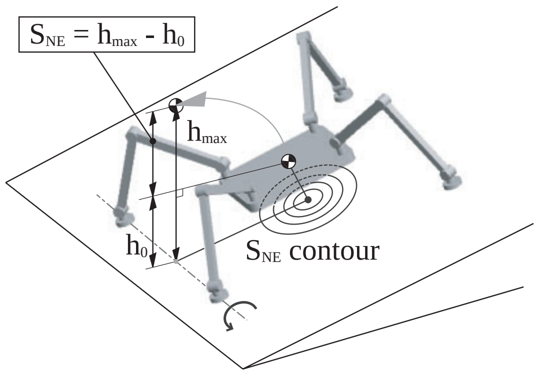

(a) Relation between normalized energy stability margin and S_{NE} contour

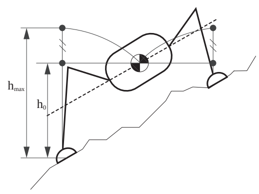

(b) Normalized energy stability margin

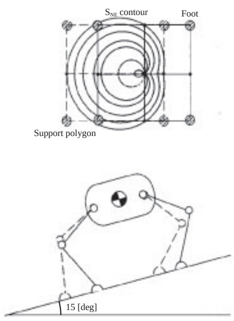

(c) Relationship between S_{NE} contour and foot positions

Fig. 4. Concept of NE stability margin and S_{NE} contour.

eration of the step over gait we derive does not depend on area reachable by a leg, and is applicable to any area reachable by a leg. Coordinates for legs and COG are described in body coordinates Σ_b and absolute coordinates Σ_w.

4. Basic Terrain-Adaptive Gait Concepts

We clarify concepts for generating a gait below.

4.1. Normalized Energy Stability Margin

To evaluate static stability in uneven terrain, we have proposed an evaluation criteria, named the normalized energy stability margin (NE stability margin) (**Fig. 4(a)**), given from the topple-over energy normalized by its own weight, and a concept of S_{NE} contour [3], lines connecting points that gives the same NE stability margin or S_{NE}. The NE stability margin is the difference in gravitational direction between the highest point and initial point on the COG trajectory if the robot topples (**Fig. 4(b)**), and is effective as a static stability evaluation criteria for a robot on uneven terrain (slope) because it is treatable geometrically. A S_{NE} contour is required for gait generation from stability that uses the NE stability margin. For a walking robot to ensure a certain NE stability margin in uneven terrain, a support polygon is formed to provide the S_{NE} contour that gives the NE stability margin (**Fig. 4(c)**). Another feature of the S_{NE} contour is to correspond to a stability margin circle for a level ground modified, for example, by the slope angle. We use this evaluation criteria, NE stability margin or S_{NE}, and the S_{NE} contour to study gait generation for ensuring stability on uneven terrain.

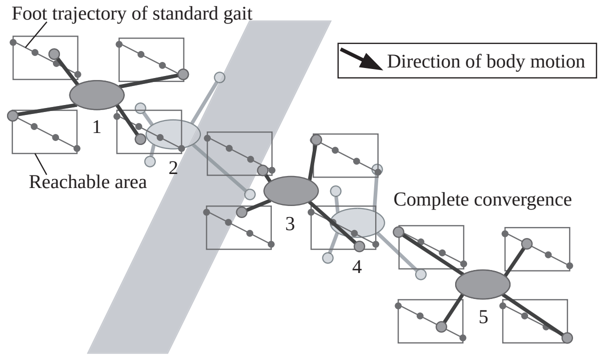

Fig. 5. Standard convergent gait [2].

4.2. Standard Convergent Gait

We have already reported [2] a standard convergent gait, i.e., a gait that is terrain-adaptive and converges to a standard gait, maintaining a certain static stability margin within a enabled-range enabled by environment conditions. **Fig. 5** is an example of a standard convergent gait showing how a walking robot makes the gait converge to the standard gait after it crossed an obstacle such as a river. We targeted improving walking continuity and reducing the number of posture transformation [4] and decided that planar gaits in the terrain-adaptive gait are to be studied based on this gait.

4.3. Unevenness-Absorbing Gait

We reported an unevenness-absorbing gait [2] (**Fig. 6**) with the standard convergent gait. Because unevenness exists on ground despite appearance, swing legs must be driven up and down to be placed at the calculated planar position regardless of unevenness. We introduced an unevenness-absorbing gait that drives swing legs up and down with a margin enabling continued smooth walking absorbing height unevenness on the ground. We found much unevenness on ground in the environment for the walking robot under development, so we decided to introduce the unevenness-absorbing gait for its height gait.

4.4. Leg Motion in Intermittent Crawl Gait

As mentioned elsewhere [5], the standard gait for static walking for more than or equal to four legs is the wave gait, which is called the crawl gait in the case of four

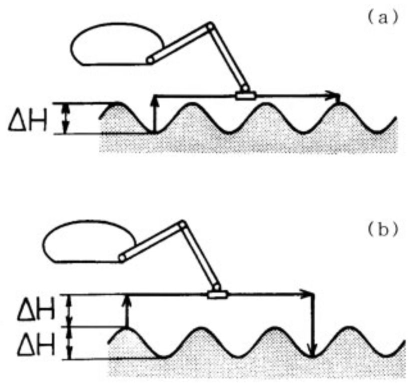

Fig. 6. Swing leg trajectory that enables to absorb unevenness ΔH of the terrain.

legs. Quadruped walking robots generally use this crawl gait. Our robot, which is used in dangerous places such as mountainous slope, is enabled with slow walking. We use our proposed intermittent crawl gait [6] as the standard gait. The intermittent crawl gait shifts COG intermittently only in the supporting phase by four legs, i.e., (1) leg r to a swing leg $\rightarrow$ (2) leg f to a swing leg $\rightarrow$ (3) COG shift $\rightarrow$ (4) leg $\bar{r}$ to a swing leg $\rightarrow$ (5) leg f to a swing leg $\rightarrow$ (6) COG shift. This is the same swing leg sequence as the crawl gait, and COG is generally shifted laterally to maximize NE stability margin. The intermittent crawl gait, which provides higher static stability among quadruped walking gaits, is suitable for a step over gait in such environments as slopes.

A robot in an intermittent crawl gait shows a zigzag COG resulting from linear swing leg motions and lateral COG shift (**Figs. 7**, **20**, **28**). This gait is achieved by driving a leg in a V shape (considering a swing leg trajectory, an isosceles triangle with a swing leg trajectory as the base (**Figs. 7(b-1)**, **(b-2)**)). This is the same as the crab gait in which the body does not face to a walking path.

4.5. Basic Policy

We used the following basic policy for determining gait generation through preliminary simulation:

(1) We achieved a continuous uneven-terrain-adaptive gait [2] by defining a period from one swing leg to the next swing leg as a step, preparing plans for the next step by calculating the next swing leg trajectory and the amount of COG shift in each step, and seamlessly connecting gait plans for each step. We decided that the gait is to be determined by cycle and that the sequence of swing legs is to be fixed to that of the standard intermittent crawl gait, i.e., leg r to a swing leg $\rightarrow$ leg f to a swing leg $\rightarrow$ leg $\bar{r}$ to a swing leg $\rightarrow$ leg f to a swing leg. If we changed the sequence for swing legs, terrain adaptation may improve. In an environment where a slope is covered with ferroconcrete and TITAN XI operates, no area exists where unsuitable footholds are densely distributed. Simulation confirmed that it gives high mobility even with a fixed swing leg sequence.

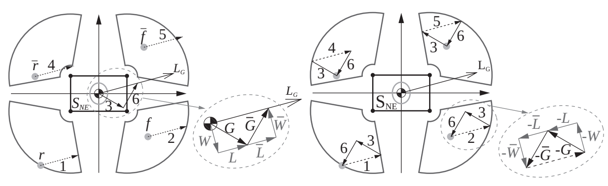

(a-1) Foot and COG trajectories in absolute coordinates

(b-1) Foot trajectories in body coordinates

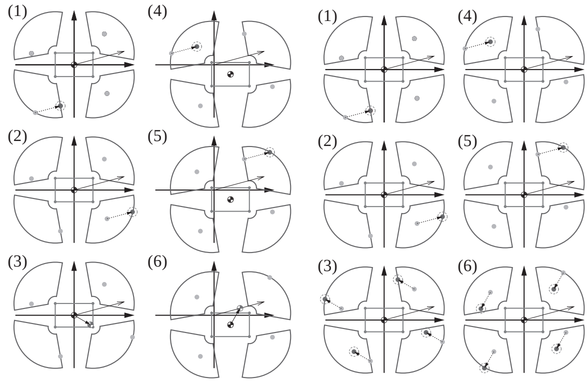

(a-2) Gait sequence in absolute coordinates

(b-2) Gait sequence in body coordinates

Fig. 7. Foot trajectories of intermittent crawl gait in the absolute and the body coordinates (the numbers in the figure show the sequence).

(2) Walking motion in next cycle C_k is derived during cycle C_{k-1} based on the gait pattern at the end of C_{k-1}, and these motions are connected to achieve smooth walking, i.e., predictively generating the next gait one cycle ahead.

(3) The amounts of COG lateral shifts to a walking path during the adaptive gait are the same within the same cycle, providing the user with intuitive, easily understood maneuvering.

(4) From energy efficiency and maneuverability, the amounts of COG lateral shifts should be minimized within the range for ensuring stability.

(5) Considering the environment, gait is determined separately for planar (*xy* plane) gait and height (*z*) gait.

Our proposed gait is somewhat specialized in stepping over ferroconcrete grids by limiting leg strokes and COG shift vectors in an intermittent crawl gait to be changed by cycle, i.e., "grid step over intermittent crawl gait", detailed below.

5. Planar (*xy*) Gait Generation

We determined a planar gait generation for the proposed grid step over intermittent crawl gait, with walking motion in cycle C_k to be determined in cycle C_{k-1}.

1. Selection of the rear leg to start the gait with (gait start)
2. The gait generation for the first half cycle (leg r to a swing leg, leg f to a swing leg, COG shift)
3. The gait generation for the second half cycle (leg $\overline{r}$ to a swing leg, leg $\overline{f}$ to a swing leg, COG shift)

Both the first and second half cycles in the intermittent crawl gait consist of a series of motions, i.e., rear leg to a swing leg → front leg to a swing leg → COG shift. The COG shift combines longitudinal and lateral shift in the direction of a walking path (**Fig. 7**). Considering these features, *xy* gait generation is made by half cycles. Gait generation for a half cycle is further divided into (1) setting foothold search area D_r for swing leg r, (2) setting foothold search area D_f for swing leg f, (3) deriving COG shift vector $\boldsymbol{G}$, and (4) determining foothold position $\boldsymbol{J}_u$.

5.1. Selection for Gait Starting Rear Leg

Swing leg motion starts with whichever rear leg is farthest to the rear from the direction of a walking path. This is because rear legs always move away from the body along the walking path. Simulation showed this simple operation to be the most effective.

5.2. Gait for First Half Cycle

5.2.1. Leg r to Swing Leg: Setting Foothold Search Area D_r

We previously proposed domain prescribing method [2] that restricts foothold search area D_u for swing legs beforehand to reduce calculation cost for foothold area searching and to avoid deadlocks. The proposed domain prescribing method used longitudinal stability margin [5] as a stability margin, which takes the shortest distance between COG on the COG shift trajectory and the sides of a support polygon, made reachable areas by a leg rectangular, and used the crawl as the standard gait. We expand this for the intermittent crawl gait using the NE stability margin. When determining the foothold position for leg r in domain prescribing method, we must consider feasibility for leg f and leg $\overline{r}$ to become swing legs after swinging of leg r. Because the step over gait we propose fixes the sequence of swing legs, we discuss leg f motion, which comes immediately after, then discuss leg $\overline{r}$ motion to become a swing leg.

First, we discuss the conditions for leg f to become the swing leg, which is the next swing motion after a swing of leg r. We have proposed domain prescribing method II for a higher convergence to the standard gait, which limits the foothold search area D_u for leg r while leg r is the swing leg so that leg f can become the swing leg thereafter. We

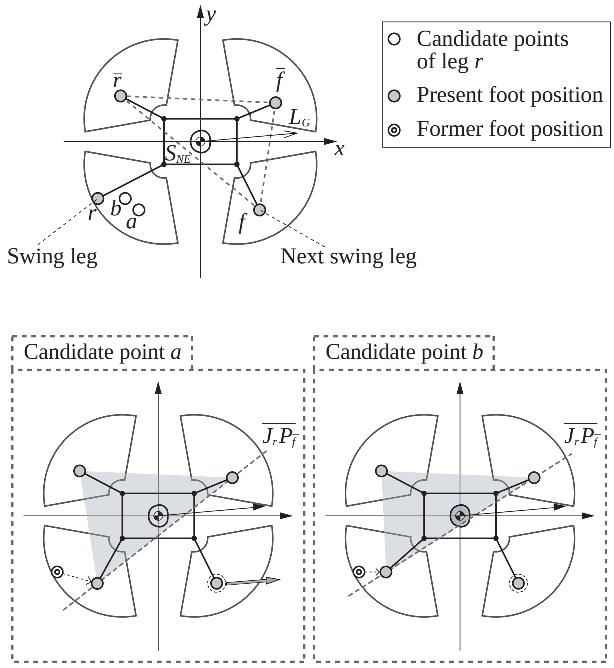

(a) Successful example of leg f swing

(b) Failed example of leg f swing

Fig. 8. Successful and failed examples of foothold on leg r for swing of leg f.

expand this and use the S_{NE} contour. **Fig. 8** indicates an example where fourth leg is swing leg r. As shown in **Fig. 8(a)**, the condition for leg f to become the swing leg while maintaining S_{NE}^c, is that diagonal support line $\overline{\boldsymbol{J}_r\boldsymbol{P}_{\overline{f}}}$ does not intersect with the S_{NE}^c contour centered by $\boldsymbol{P}_g$ after leg r is placed. This is achieved by placing leg r in the domain before the tangential line from leg f to the S_{NE}^c contour.

Then, we discuss the conditions for leg $\overline{r}$ to become the swing leg, which is the swing motion after swings of leg r and f. We have reported that the feasibility for leg $\overline{r}$ to become the swing leg is determined two steps before when the foothold position for leg r is determined. This is because diagonal support line $\overline{\boldsymbol{J}_r\boldsymbol{P}_{\overline{f}}}$ affects leg $\overline{r}$ to become the swing leg. We proposed domain prescribing method I, which restricts the foothold search area D_u for leg r when leg r is the swing leg considering the limit of area reachable by leg $\overline{r}$, two steps after. Domain prescribing method I considers areas reachable by leg $\overline{f}$, leg $\overline{r}$, and the leg r itself for swing leg r, and to provide foothold search area D_u for swing leg r by formulating these restrictions using the longitudinal stability margin. Restricting foothold search area D_u using the S_{NE} contour would result in high calculation cost and complication in setting the foothold search area for leg r due to the area reachable by leg r itself. We thus consider both COG shift vector modification and setting the foothold search area D_u for leg r at the same time. **Fig. 9** is an example where the fourth leg is swing leg r, as in **Fig. 8**. Note that leg $\overline{r}$ starts the swing immediately after the COG shift, so we must derive COG

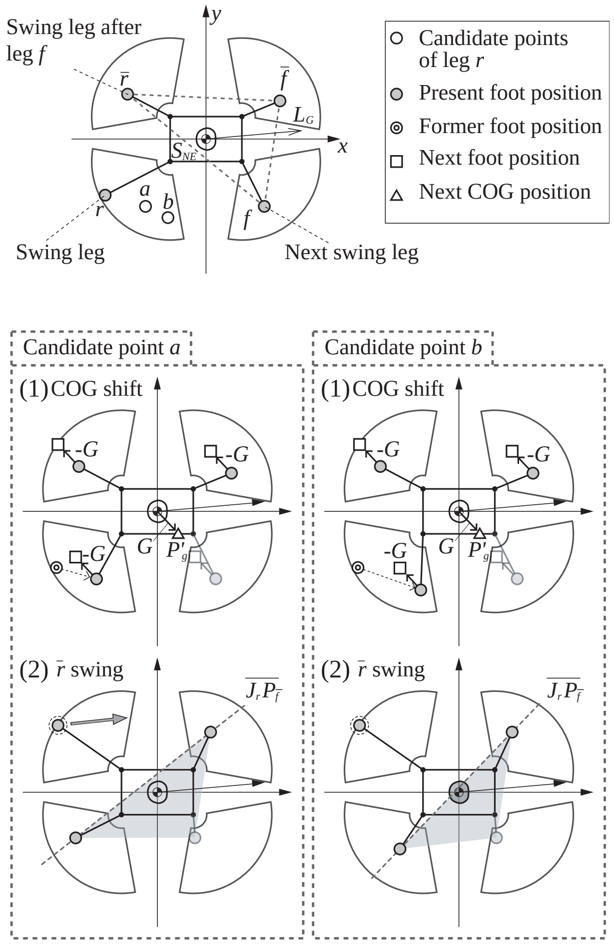

(a) Successful example of leg $\bar{r}$ swing

(b) Failed example of leg $\bar{r}$ swing

Fig. 9. Successful and failed examples of foothold on leg r for swing of leg $\bar{r}$.

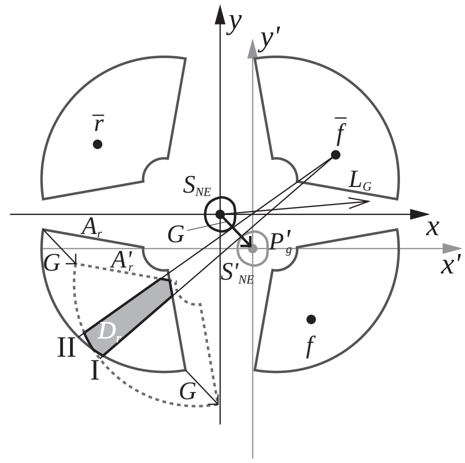

Fig. 10. Domain prescribing method for rear leg in the case of intermittent crawl gait.

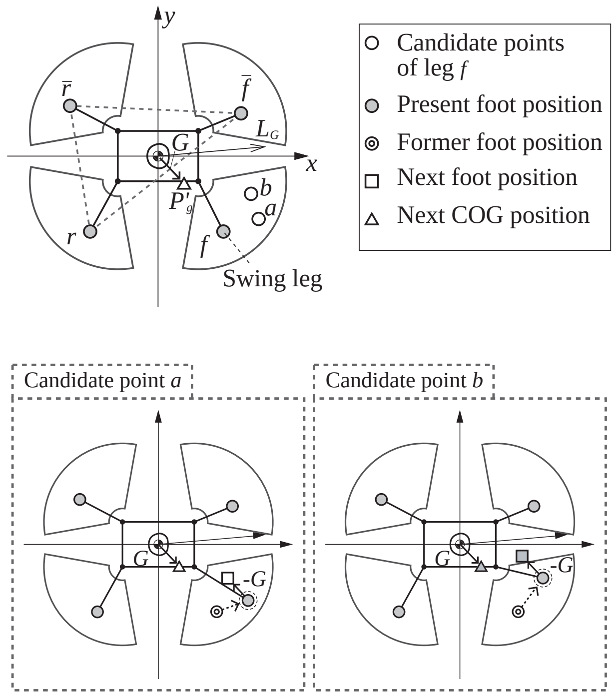

(a) Successful example of COG shift

(b) Failed example of COG shift

Fig. 11. Successful and failed examples of foothold on leg f for COG shift.

shift vector $\boldsymbol{G}$ using the method in Section 5.2.3. Using the COG shift vector, COG position $\boldsymbol{P}'_g$ after the COG shift is given. As shown in **Fig. 9(a)**, the condition for leg $\bar{r}$ to become the swing leg while maintaining S^c_{NE} is that diagonal support line $\overline{\boldsymbol{J}_r\boldsymbol{P}_{\bar{f}}}$ does not intersect with the $S^{c'}_{NE}$ contour centered by $\boldsymbol{P}'_g$. This is ensured by placing leg r in the domain after the tangential line from leg $\bar{f}$ to the $S^{c'}_{NE}$ contour after COG is moved by vector $\boldsymbol{G}$.

The above two conditions, which enable leg f and leg $\bar{r}$ to become swing legs after the completion of leg r motion as a swing leg, are equivalent to taking foothold search area D_r (**Fig. 10**) embraced by the two tangential lines, reachable area A_r, and A'_r after the COG shift. Actual foothold position $\boldsymbol{J}_r$ is determined in Section 5.3.

5.2.2. Leg f to Swing Leg: Setting Foothold Search Area D_f

Since the COG shift, which takes place immediately after leg f is swung, has been determined, $\boldsymbol{J}_f$ should be selected at a position that does not disturb the COG shift by COG shift vector $\boldsymbol{G}$ (**Fig. 11**). So, $\boldsymbol{P}'_f = \boldsymbol{P}_f - \boldsymbol{G}$, where $\boldsymbol{P}'_f$ is the position of leg f after the COG shift, must be within reachable area A_f.

As shown in **Fig. 12**, foothold search area D_f is equivalent to the common area of reachable area A_f and reachable area A'_f after the COG shift. As with leg r, the actual foothold position of swing leg f is also determined in Section 5.3.

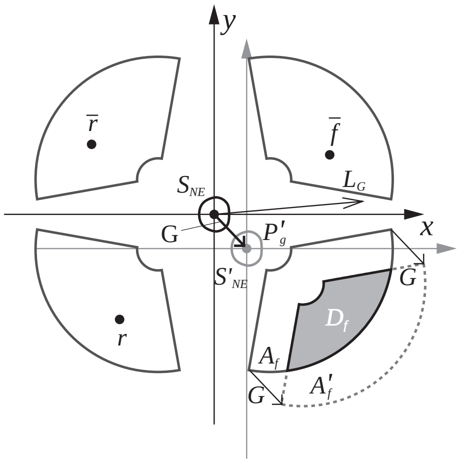

Fig. 12. Domain prescribing method for front leg in the case of intermittent crawl gait.

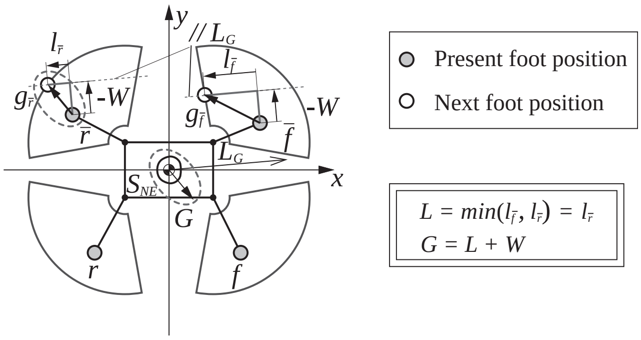

Fig. 13. Calculation of COG shift vector **G** with considering the reachable area of leg $\bar{f}$ and $\bar{r}$.

5.2.3. COG Shift: Deriving COG Shift Vector $\boldsymbol{G}$

The COG shift is determined considering areas reachable by four legs and the instructed walking path. There is a phase difference of a half cycle for the left and right legs in the intermittent crawl gait, and leg motion in different phases should not obstruct leg motion on the opposite side. COG shift vector $\boldsymbol{G}$ is obtained based on restrictions on reachable areas for leg $\bar{f}$ and leg $\bar{r}$.

As shown in **Fig. 7**, the COG shift vector is expressed by the sum of COG lateral vector $\boldsymbol{W}$ in the direction lateral to a walking path, and COG longitudinal vector $\boldsymbol{L}$ in the walking path. For vector $\boldsymbol{W}$, we use standard COG shift vector $\boldsymbol{W}_{std}$ as initial COG lateral vector. Since the COG lateral vector and walking path were determined, it is possible to calculate planar moving distance of supporting leg $\boldsymbol{l}_i$, in the opposite direction from the walking path L_G, which is restricted by reachable areas of legs. As shown in **Fig. 13**, $\boldsymbol{l}_i$ indicates each distance from a leg position after $-\boldsymbol{W}$ motion to the position where leg i is moved in the direction opposite L_G until it is restricted by the reachable area. Thus, $|\boldsymbol{L}|$ which is the length of $\boldsymbol{L}$ and COG longitudinal distance in the walking path is; $|\boldsymbol{L}| = \min(|\boldsymbol{l}_{\bar{f}}|, |\boldsymbol{l}_{\bar{r}}|)$. With this, COG shift vector $\boldsymbol{G}$ is obtained by, $\boldsymbol{G} = \boldsymbol{L} + \boldsymbol{W}$. The distance of walking in L_G by $\boldsymbol{L}$ is limited to not exceed walking distance based on $\boldsymbol{L}_{std}$ of the standard gait. This comes from the waking distance of the standard gait. When $\boldsymbol{L}$ or $\boldsymbol{W}$ is changed, $\boldsymbol{G}$ is recalculated.

If $\boldsymbol{J}_r$ and $\boldsymbol{J}_f$ can not be determined using $\boldsymbol{G}$, obtained considering the reachable area for leg $\bar{f}$ and leg $\bar{r}$ on the opposite side, the following modifications (a) and (b) are added to $\boldsymbol{G}$:

(a) $\boldsymbol{J}_r$ cannot be placed within D_r

1. Repeat the search for $\boldsymbol{J}_r$ with increased COG lateral vector $\boldsymbol{W}$ by a certain amount until $\boldsymbol{J}_r$ is able to be placed.

2. If the increase in lateral shift exceeds a certain value before $\boldsymbol{J}_r$ is determined, return to (1) and repeat the search for $\boldsymbol{J}_r$ with decreased $|\boldsymbol{L}|$ of COG longitudinal vector $\boldsymbol{L}$. COG lateral vector $\boldsymbol{W}$ is reset to $\boldsymbol{W}_{std}$.

(b) $\boldsymbol{J}_f$ cannot be placed within D_f

When $\boldsymbol{J}_f$ can not be determined, return to the setting D_r with increased COG lateral vector $\boldsymbol{W}$ by a certain amount and repeat setting D_r and the search for $\boldsymbol{J}_r$.

5.3. Determining Foothold Position $\boldsymbol{J}_u$ in Foothold Search Area

For searching for a foothold position, initial foothold-search position $\boldsymbol{I}_u$ is first determined and actual foothold position $\boldsymbol{J}_u$ is derived through searching within the search area. In conjunction with deriving an initial foothold-search position $\boldsymbol{I}_u$, we propose "phase-reserved positioning method" [2] to ensure converging to a standard convergent gait in the crawl gait. Phase-reserved positioning focuses on the position of leg u^*, the swing leg one step before swing leg u in the standard gait. The initial foothold-search position $\boldsymbol{I}_u$ for leg u is set to the position, on the standard stroke of leg u, distant from the return start position of leg u in the standard gait by the distance of the stride (phase difference) of the leg u^* in the support leg phase. This is because if leg u^* returned to the return end point of the standard gait, the positional relationship between leg u and leg u^* is matched by the standard gait pattern to converge at the standard gait. We expand this to be applied to the intermittent crawl gait.

In the grid step over intermittent crawl gait, the relative leg trajectory of the standard crab gait on the *xy* plane is V shaped (considering a swing leg trajectory, an isosceles triangle with a swing leg trajectory as the base) (**Fig. 7**). The COG shift in the instructed walking path is equal to swing leg stroke length ($|\boldsymbol{L}_{std}| + |\bar{\boldsymbol{L}}_{std}| = 2|\boldsymbol{L}_{std}|$). With this, we decided that initial foothold-search position $\boldsymbol{I}_u$ for swing leg $\bar{r}$ is to be determined considering stride distance Δs of leg $\bar{f}$ and the return start point of the standard gait as shown in **Fig. 14(a)**, and that initial foothold-search position $\boldsymbol{I}_u$ for swing leg f is to be determined similarly considering stride distance Δs of leg r and the return start point of the standard gait as shown in **Fig. 14(b)**.

If $\boldsymbol{I}_u$ cannot be obtained on the trajectory of the swing leg stroke (e.g., the distance between $\boldsymbol{I}_u$ and the return start point is bigger than the stroke of the standard gait, or

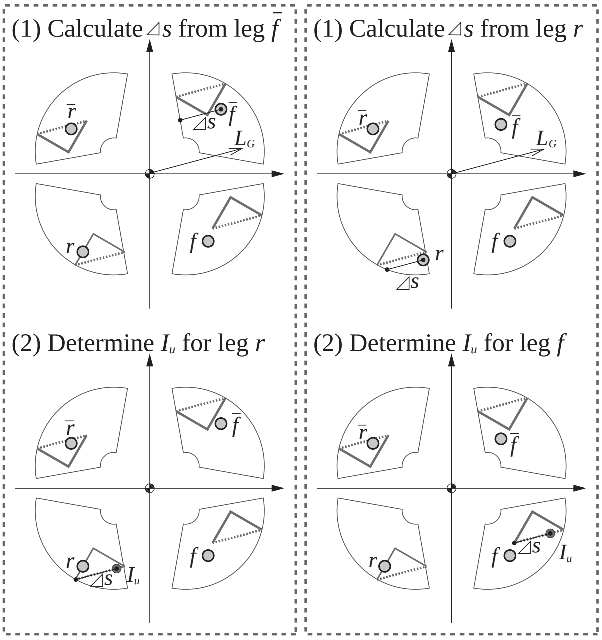

(a) I_u of leg r for phase-reserved positioning method

(b) I_u of leg f for phase-reserved positioning method

Fig. 14. Phase-reserved positioning method in the case of intermittent crawl gait.

at the beginning of walking), the return end point of the standard gait is assigned as $\boldsymbol{I}_u$. The concrete way to select an actual foothold position $\boldsymbol{J}_u$ in foothold search area D_u from the initial foothold-search position $\boldsymbol{I}_u$ is:

1. If $\boldsymbol{I}_u$ is suitable as a foothold position judging from map information, the point is set to the foothold position. If not, the procedure below is followed.

2. Points in foothold search area D_u are examined for whether they are suitable for foothold position, in the $+y$ and $-y$ direction equidistantly from the position closest to $\boldsymbol{I}_u$.

3. If procedure (2) does not provide the solution, the search row is moved in the $-x$ direction and procedure (2) is repeated. The initial search point of this row is set on the swing leg stroke line of the standard gait. If it still does not provide a solution, the search row is moved from $\boldsymbol{I}_u$ equidistantly to the $+x$ direction, and the procedure (2) is repeated. The process is repeated until $\boldsymbol{J}_u$ is found.

5.4. Flow of Gait Generation for Half Cycle

As mentioned earlier about the *xy* gait generation, the *xy* gait generation is conducted in major steps: (1) selection of the rear leg for starting the gait, (2) gait generation for the first half cycle, (3) gait generation for the second half cycle and (4) confirmation of COG shift. Half cycle gait generation for (2) and (3) is conducted (**Fig. 15**) in the following steps: (1) deriving the COG shift vector, (2) setting the foothold search area for the rear leg, (3) determining the initial foothold search position for the rear leg,

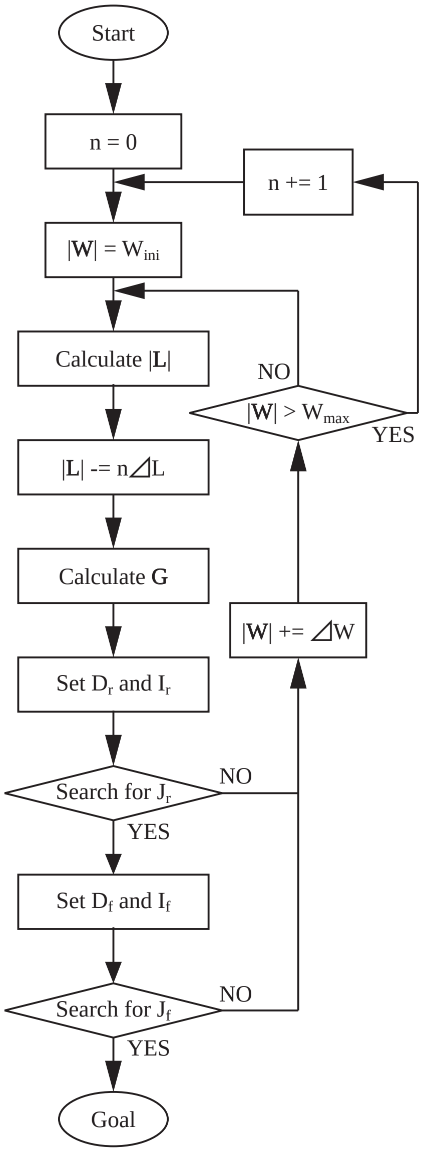

Fig. 15. Flow chart for gait generation for a half cycle.

(4) determining the foothold position for the rear leg, (5) setting the foothold search area for the front leg, (6) determining the initial foothold search position for the front leg, and (7) determining the foothold position for the front leg. When robots actually walk, limitations may be set on search time and COG longitudinal distance.

5.5. Gait for Second Half Cycle: Confirmation of COG Shift Vector

With the steps above, the first half cycle gait is obtained. The second half cycle gait is then determined. Gait generation for the second half cycle is basically the same as in the first half, and is determined by deriving $\boldsymbol{J}_{\bar{r}}$, $\boldsymbol{J}_{\bar{f}}$, $\bar{\boldsymbol{G}}$. If the second half cycle gait does not meet the condition of the S^c_{NE} contour with COG shift vector $\bar{\boldsymbol{G}}$ given by COG lateral vector $\bar{\boldsymbol{W}}$ whose moving distance is the same as that of $\boldsymbol{W}$ in the first half cycle, i.e., $|\boldsymbol{W}| \neq |\bar{\boldsymbol{W}}|$, the process returns to gait generation for the first half cycle and tries again with an increased COG lateral shift

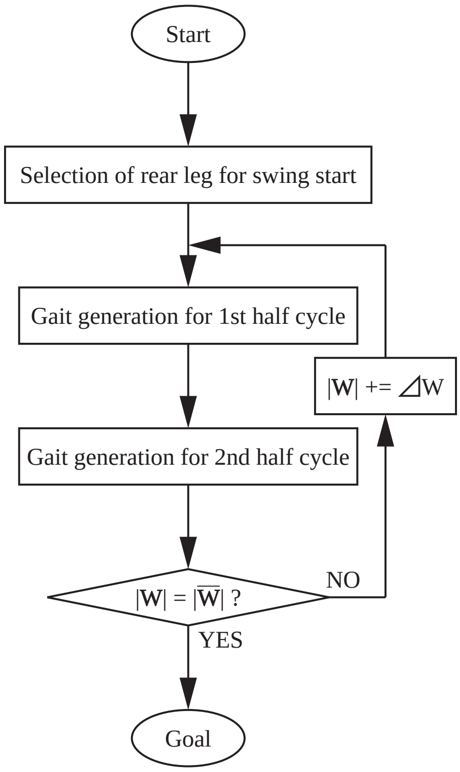

Fig. 16. Flow chart for *xy* gait generation.

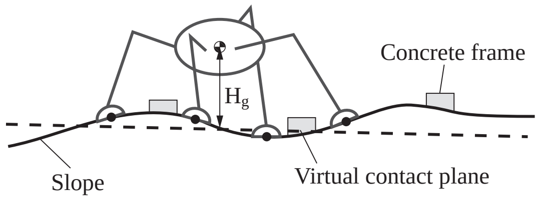

Fig. 17. Virtual contact plane.

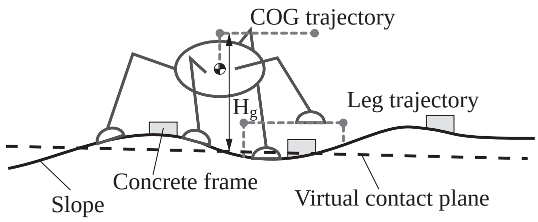

Fig. 18. Swing leg trajectory for *z* gait generation.

vector $\boldsymbol{W}$ to make distances of left and right COG lateral shift the same in a cycle to follow a walking path L_G, and to provide the user with intuitive and easily understood maneuvering. Gait generation for one cycle is shown in **Fig. 16**.

6. Height (*z*) Gait Generation

Determining the foothold position on the *xy* plane was derived in the previous section. A leg trajectory considering the height of COG and swing legs is generated as follows:

6.1. Generating Virtual Contact Plane and Deriving S_{NE} Contour

If the four legs of walking robots moving in environments are not on the same plane due to terrain unevenness, the S_{NE} contour must be reexamined, so we derive a "virtual contact plane" to draw a S_{NE} contour, in which the four supporting legs are assumed to be on the same plane virtually (**Fig. 17**). We derive the contact plane by simply approximating the *z* position of the four legs with the least squares method, so the virtual contact plane is used as the *xy* plane and the direction perpendicular to the plane is used as the *z* direction for generating a gait.

6.2. Determining the Height of the Swing Leg Foothold Position

The height of the foothold position J_{uz} of swing leg u is derived by selecting the height on the map at the position corresponding to J_{ux} and J_{uy} of foothold position $\boldsymbol{J}_u$ derived in *xy* gait generation.

6.3. COG Height Determination

To determinate the height of P_{gz} of COG from the view of user maneuverability, we make the robot to go forward horizontally along the surface of terrain keeping a constant height insofar as possible. We thus decided that COG height P_{gz} be set to a point higher by H_g from the virtual contact plane obtained above using map information within providing the S_{NE} contour. In actual operation, adjustments may be needed such as adopting larger H_g to avoid contact with raised portions when operating on extremely uneven terrain.

6.4. Generating Trajectory

As mentioned above, height gait generation is based on the unevenness-absorbing gait. We set a trajectory (**Fig. 18**) assuming that (1) the walking robot is large and heavy, and that (2) safety has priority. Note that no relationship exists between the leg and COG velocity because swing leg motion and the COG shift are mutually independent in the intermittent crawl gait. Unlike the crawl gait, velocity for these swing legs and COG shift is set independently.

6.4.1. Swing Leg Trajectory

The leg trajectory is rectangular (up phase: vertical ascending, return phase: horizontal motion, down phase: vertical descending) to reliably and safely avoid obstacles (frames). Unlike the crawl gait, COG remains stationary during leg swinging to give a rectangular trajectory for both Σ_w and Σ_b. The return distance is obtained by $\boldsymbol{J}_u - \boldsymbol{P}_u$. The ascending distance is determined to ensure enough height from the virtual contact plane to avoid frames in the return trajectory. The descending distance is derived based on J_{uz} of the foothold position $\boldsymbol{J}_u$.

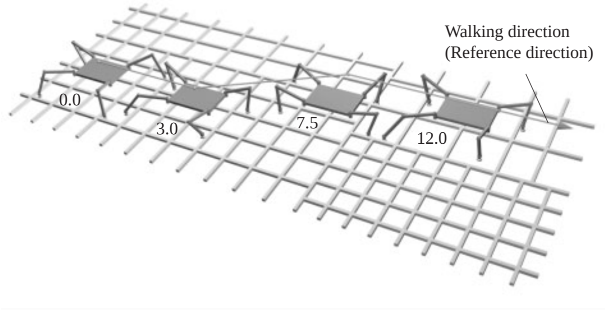

Fig. 19. Simulation of step over walking motion while changing of the walking direction (the numbers in the figure show the cycle).

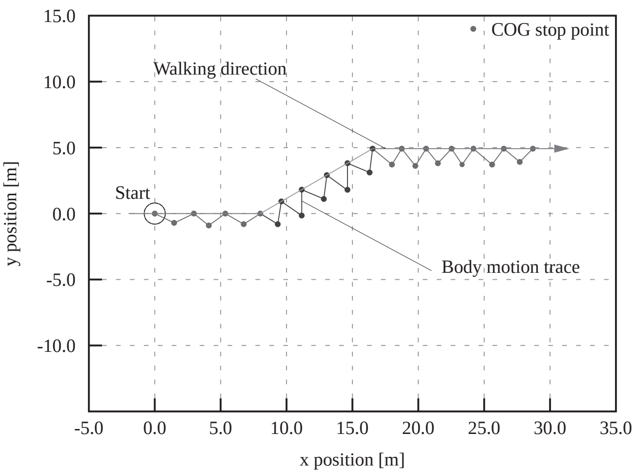

Fig. 20. The COG trace of a quadruped walking robot in **Fig. 19**.

6.4.2. COG Trajectory

Since COG height P_{gz} is constant during a cycle, COG is moved in the z direction before a xy gait until it reaches P_{gz}, and the xy gait starts with height H_g maintained.

7. Verification by Simulation

Using simulation, we verified the validity of gait control discussed above. Simulation was conducted with ferroconcrete frames 200 mm and 300 mm square with grids of 2.0 m and 3.0 m, considering environmental conditions common at actual construction sites where the robot actually works. And assuming environments combining these conditions, we confirmed that the robot walks in all directions without a problem (**Figs. 19** and **20**).

Figure 19 shows how the robot first moves straight and avoids the concrete frame-packed areas ahead of it by changing the walking path (direction). Although the walking path was given through instructions from a user, we confirmed that the robot can continue walking following these instructions by generating terrain-adaptive gaits. **Fig. 20** shows the COG trace and instructed walking path (direction). Although the COG trajectory deviates once from the instructed trajectory due to the COG lateral shift, a characteristic of the intermittent crawl gait, we confirmed that COG returns to the instructed trajectory upon completion of each cycle.

Fig. 21. Overview of constructed TITAN XI.

Table 1. Specifications of TITAN XI.

Size	4.8 [m] × 5.0 [m] × 3.0 [m]
Leg length	3.7 [m]
Mass	7,000 [kg]
Power	41.9 [kW]

8. Walking Experiment with Mechanical Model TITAN XI

8.1. Quadruped Walking Robot TITAN XI for Steep Slope Operation

We verified gait control using TITAN XI (**Fig. 21**, **Table 1**).

TITAN XI legs have 3 DOF driven by hydraulic cylinders, a drill in the middle of the body, two winches in the back to reel tethers pulling the robot, two crawlers at the bottom for secondary motion, an engine at left, and electronic components such as a PC at right. The PC uses 3 PC104plus-compatible onboard computers (CPU: NS-Geode 300 MHz, Compact Flash Disk: 512 MB, Memory: 256 MB, LAN Device, OS: Linux). TITAN XI also uses 2 DOF tethered system [1] to improve walking by controlling tether tensions, offsetting the parallel component on the slope of gravity of the robot, leaving the perpendicular component by controlling two-tether tensions. By controlling combined tether tensions equal to the parallel component of the slope of gravity, the robot moves omnidirectionally on the slope. TITAN XI uses a commercially available controller (joystick) for construction machines to generate instructions for remote control, e.g., of walking (direction and speed), drilling, and direct control in an emergency.

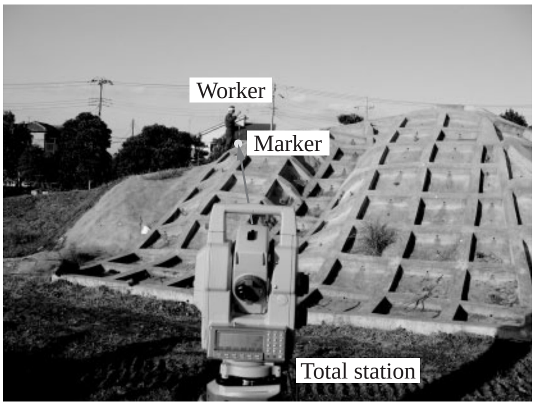

Fig. 22. Concept of terrain measurement.

8.2. Map Generation: Terrain Measurement and Self-Localization

Walking robots must obtain environmental information for generating motions adapted to the terrain.

Ways of doing this include processing images taken by cameras [7] or distance measured by Laser Range Finders (LRFs) [8]. These have problems for use outside, however. Image processing, for example, does not provide precise environmental information despite the advantage of quick measurement, and LRFs require much calculation time despite the precise information they obtain. A walking robot must know its own precise position to use map information. Conventional self-localization generally obtains information using Global Positioning System (GPS) or measuring multiple landmarks. GPS may have difficulty receiving signals from GPS satellites in mountainous areas, and landmarks must be placed on the ground.

The slopes where TITAN XI operates involves a poor environment that exposes sensors to dirt and dust, so sensors require extra protection such as a wiper to ensure that they operate properly. So we decided that no sensors are mounted on the robot.

We studied terrain measurement and self-localization method for TITAN XI using measurement devices, introducing established reliable surveying, eventually using automatic tracking, Total Station (TS; TOPCON). TS features (1) a kilometer-long survey range, (2) high measurement precision ($\pm$ 5 mm 3D positioning precision), and (3) automatic search and tracking for corner cubes.

8.2.1. Introducing Terrain Measurement Using Surveying

Terrain measurement using TS is done (**Fig. 22**) by placing corner cubes (total reflection prisms) at intersections of concrete frames and at points on the ground surrounded by frames on the slope and measuring them with 3D measurement by operators before construction works using the robot as follows:

1. Measuring coordinates at intersections of frames and at each point close to centers of areas surrounded by frames.

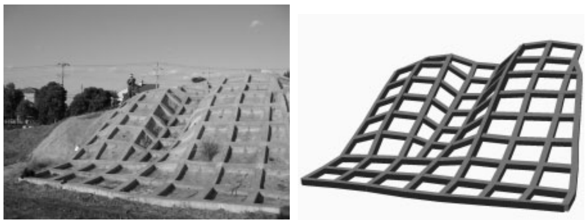

(a) Real slope (b) Modeled slope

Fig. 23. Real slope and modeled slope.

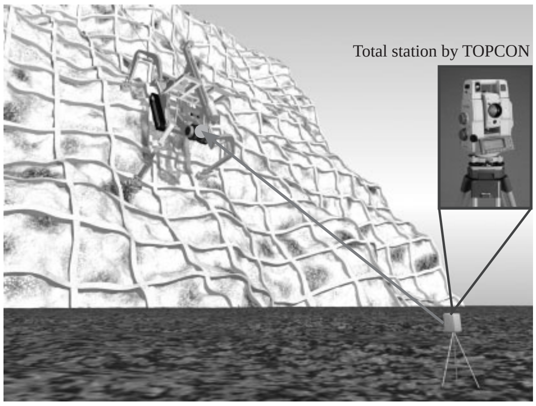

Fig. 24. Concept of self-localization.

2. Modeling frames by connecting intersections as center lines and adding frame design information (width and height), obtaining normal vectors for local planes formed by measured points, defined as the frame height direction.

3. Modeling for the slope by combining coordinates of points close to centers of areas surrounded by frames and frame modeling information obtained in the previous step.

4. Generating two maps, i.e., an unevenness grid map, which records height information on the slope from a certain base plane in cells, and a forbidden foothold grid map, which records unsuitable footholds (e.g., frames, uneven parts too big to be absorbed by leg motion) in cells.

Figure 23 shows modeling results of the real slope using our proposal and confirmed that we obtained geometric information on the terrain sufficient for the robot to walk, although the proposal is based on easy measurements and a simple algorithm.

8.2.2. Introduction of Self-Localization Using Surveying

Self-localization of the robot with TS were conducted using the same TS used in environment modeling, placing a corner cube on the robot to be tracked in real time, installing and using information on a single-axis attitude sensor on the robot (**Fig. 24**).

Fig. 25. Rotating mechanism for self-localization.

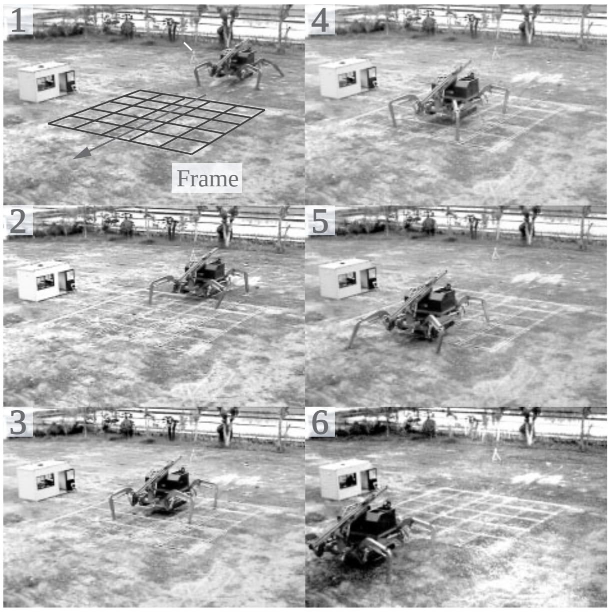

Fig. 26. Serial motion of TITAN XI to make the terrain adaptive walking over the dummy frames.

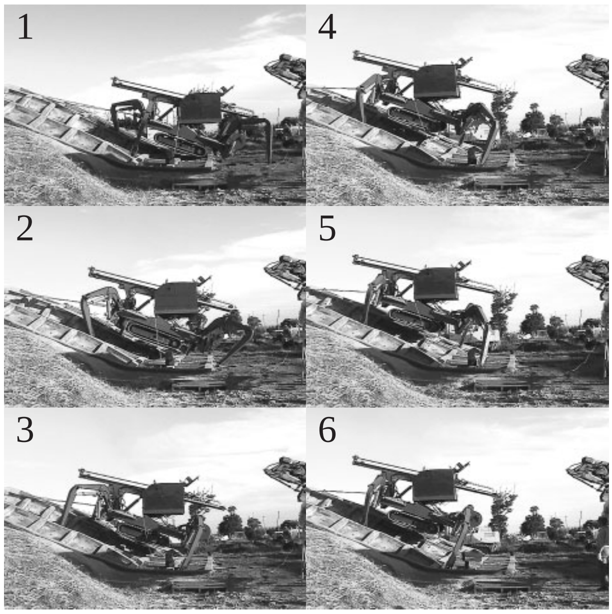

Fig. 27. Snapshots of walking experiment on a test slope covered with concrete frames.

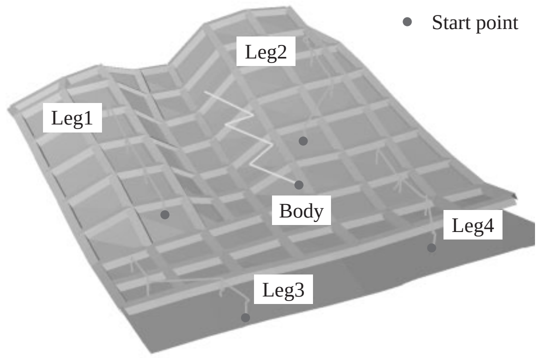

Fig. 28. Body and leg traces of TITAN XI in **Fig. 27**.

The corner cube for the robot is installed on a rotating mechanism (**Fig. 25**) that rotates the cube with a certain radius, and is tracked automatically by TS on the ground to measure coordinates of three arbitrary points on the circumference in a certain period. With these coordinates of the three points, both the coordinates of the rotating center and the vector indicating the axis direction of rotation are derived. Using this information with additional information from the single-axis attitude sensor, the pose of the robot can be identified.

8.3. Walking Experiment with Dummy Frames on Planar Ground

To verify the functions of our proposed terrain-adaptive gait and map generation, we conducted a walking experiment (**Fig. 26**) in a dummy frame area using ropes for a concrete frame area on a slope.

The experiment field is a plane 30 m $\times$ 5 m including frames of 0.2 m $\times$ 0.2 m a size often used on the slopes where TITAN XI is to work. Map information for the experimental field was generated by our proposed map generation. In an experiment where TITAN XI entered straight and passed through, we confirmed the generation of leg motion to avoid contact with frames with static stable walking and the gait converged at the standard gait once the robot went through the frame area. Through this walking experiment, we demonstrated the feasibility of our proposal for practical models.

8.4. Walking Experiment on Test Slope

We conducted a slope walking experiment with TITAN XI on a small slope as a comprehensive experiment for the mechanism and control we developed and as a preliminary experiment viewing practical use. The slope had a maximum inclination of 30°, concrete frames of 1.5 m intervals on both sides, and a height and width of 0.2 m. The surface is paved with mortar with sufficient strength. We ensured safety by pulling TITAN XI with tethers.

Figure 27 shows the experiment and **Fig. 28** the COG and leg traces. We confirmed that TITAN XI climbed the slope avoiding the ferroconcrete frames. Although this slope is more moderate than that assumed for TITAN XI in practical use, the robot generated the expected motion and achieved continuous stable walking and the mechanism and control algorithm functioned smoothly. These facts demonstrated the usability of the grid step over intermittent crawl gait we proposed and the possibility of developing this system much further.

9. Conclusions

We have discussed gait control for quadruped walking robots that enables stable and continuous walking on slopes covered with ferroconcrete frames where wheeled vehicles or crawlers have difficulty operating. We proposed varying COG shift and foothold positions in generating gaits based on the intermittent crawl gait and map generation expanded from surveying. We made computer simulation and walking experiments using a mechanical model TITAN XI for verifying the feasibility. As discussed above, TITAN XI, a quadruped walking robot, achieved a further step toward practical use on slopes through this work.

Practical use of TITAN XI at actual construction sites will require the following:

- Study on actual slopes involving concrete frames and uneven terrain.
- A long-distance walking experiment with pose corrected by the proposed self-localization.
- A study for gait control to optimize the attitude of a walking robot based on terrain.

We will continue working on these technical issues to realize a practical machine.

Acknowledgements

This study was funded by a matching fund from Ministry of Economy, Trade, and Industry of Japan.

References:

[1] R. Hodoshima et al., "Development of TITAN XI: a Quadruped-Walking Robot to Work on Slopes – Design of system and mechanism," Proceedings of IEEE/RSJ International Conference on Intelligent Robots and Systems, pp. 792-797, August, 2004.

[2] S. Hirose et al., "The Gait Control System of a Quadruped Walking Vehicle," Advanced Robotics, Vol.1, No.4, pp. 289-323, 1986.

[3] S. Hirose et al., "Normalized Energy Stability Margin and its Contour of Walking Vehicles on Rough Terrain," Proceedings of International Conference on Robotics and Automation, pp. 181-186, May, 2001.

[4] S. Hirose and K. Yokoi, "The Standing Posture Transformation Gait of a Quadruped Walking Vehicle," Advanced Robotics, Vol.2, No.4, pp. 345-359, 1988.

[5] R. B. McGhee and A. A. Frank, "On the stability properties of quadruped creeping gaits," Mathematical Biosciences, Vol.3, pp. 331-351, 1968.

[6] H. Tsukagoshi and S. Hirose, "Intermittent crawl gait for quadruped walking vehicles on rough terrain," Proceedings of International Conference Climbing and Walking Robots, pp. 323-328, November, 1998.

[7] R. Volpe et al., "Enhanced Mars Rover Navigation Techniques," Proceedings of International Conference on Robotics and Automation, pp. 926-931, April, 2000.

[8] E. Krotov and R. Hoffman, "Terrain mapping for walking planetary rover," IEEE Transactions on Robotics and Automation, Vol.6, No.10, pp. 728-739, 1994.

Name:
Ryuichi Hodoshima

Affiliation:
Research Fellow, Department of Mechanical and Aerospace Engineering, Tokyo Institute of Technology

Address:
2-12-1 Ookayama, Meguro-ku, Tokyo 152-8552, Japan

Brief Biographical History:
2006 Received Doctor of Engineering in Mechanical and Aerospace Engineering from Tokyo Institute of Technology
2006- Research Fellow, Department of Mechanical and Aerospace Engineering, Tokyo Institute of Technology

Main Works:
• "Development of Quadruped Walking Robot TITAN XI for Steep Slopes –Slope Map Generation and Map Information Application–," Journal of Robotics and Mechatronics, Vol.18, No.3, pp. 318-324, 2006.
• "Development of a Quadruped Walking Robot TITAN XI for Steep Slopes Operation –Conceptual Design and Basic Experiment of Leg Driving Mechanism–," Journal of Robotics Society of Japan, Vol.23, No.7, pp. 847-857, 2005 (in Japanese).

Membership in Academic Societies:
• The Robotics Society of Japan (RSJ)

Name:
Takahiro Doi

Affiliation:
Research Associate, School of Life System Science and Technology, Chukyo University

Address:
101 Tokodachi, Kaizu-cho, Toyota-shi, Aichi 470-0393, Japan

Brief Biographical History:
2003 Received Ph.D. Degree in Department of Control Engineering, Tokyo Institute of Technology
2003- Researcher, TLO, Tokyo Institute of Technology (The Circle For The Promotion Of Science And Engineering)
2005- Research Associate, School of Life System Science and Technology, Chukyo University

Main Works:
• "Development of Quadruped Walking Robot TITAN XI for Steep Slopes –Slope Map Generation and Map Information Application–," Journal of Robotics and Mechatronics, Vol.18, No.3, pp. 318-324, 2006.
• "Study of Shape Representation Using Internal Radiated-light Projection Method," Journal of Robotics Society of Japan, Vol.21, No.4, pp. 427-435, 2003.
• "3D Visual Information Processing and Gait Control of a Quadruped Robot," Journal of Robotics and Mechatronics, Vol.15, No.3, pp. 349-355, 2003.

Membership in Academic Societies:
• The Robotics Society of Japan (RSJ)
• The Society of Instrument and Control Engineers (SICE)

Name:
Yasushi Fukuda

Affiliation:
Associate Professor, Department of Mechanical Systems, Faculty of Engineering, Tamagawa University

Address:
6-1-1 Tamagawagakuen, Machida-shi, Tokyo 194-8610, Japan

Brief Biographical History:
1985 Joined Toshiba Corporation
2002- Senior Research Scientist, TLO, Tokyo Institute of Technology (The Circle For The Promotion Of Science And Engineering)
2005- Associate Professor, Department of Mechanical Systems, Faculty of Engineering, Tamagawa University

Main Works:
• "The Gait Control System of the Quadruped Wa1king Vehicle," Advanced Robotics, Vol.1, No.4, pp. 289-323, 1986.
• "Sensor-based proximity operation of an astronaut reference robot," Advanced Robotics, Vol.9, No.7, pp. 653-673, 1995.
• "Assembly Experiment of microsatellite by space maintenance robot," The 6th International Symposium on Artificial Intelligence, Robotics and Automation in Space (i-SAIRAS), June, 2001.

Membership in Academic Societies:
• The Robotics Society of Japan (RSJ)
• The Society of Instrument and Control Engineers (SICE)
• The Japan Society of Mechanical Engineers (JSME)

Name:
Shigeo Hirose

Affiliation:
Dr. Eng. Professor, Dept. of Mechanical & Aerospace Engineering, Tokyo Institute of Technology

Address:
I1-52, 2-12-1 Ookayama, Meguro-Ku, Tokyo 152-8552, Japan

Brief Biographical History:
1976 Received Dr. Eng. degree in Mechanical Engineering Science from Tokyo Institute of Technology, Japan
1992- Professor in Tokyo Institute of Technology
2006 Medal with Purple Ribbon

Main Works:
• Creative Design of Robots
• Rescue Robots
• Humanitarian Demining Robots
• "A New Approach to Humanitarian Demining Part1: Mobile Platform for Operation on Unstructed Terrain," Autonomous Robots, Vol.18, pp. 303-324, 2005.
• "Helios VII: A New Vehicle for disaster response-mechanical design and basic experiments," Advanced Robotics, Vol.19, No.8, pp. 901-927, 2005.
• "Biologically Inspired Robot," Oxford University Press, 1993.

Membership in Academic Societies:
• IEEE Fellow, Robotics and Automation Society
• The Japan Society of Mechanical Engineers (JSME) Fellow
• The Robotics Society of Japan (RSJ) Fellow

Name:
Toshihito Okamoto

Affiliation:
CEO of Taisho Kensetu Corporation

Address:
2695 Kaneda, Chosei-mura, Chosei-gun, Chiba 299-4332, Japan

Brief Biographical History:
1973- Started Taisho Kensetu Corporation

Main Works:
• "Development of Quadruped Walking Robot TITAN XI for Steep Slopes –Slope Map Generation and Map Information Application–," Journal of Robotics and Mechatronics, Vol.18, No.3, pp. 318-324, 2006.
• "Development of a Quadruped Walking Robot TITAN XI for Steep Slopes Operation –Conceptual Design and Basic Experiment of Leg Driving Mechanism–," Journal of Robotics Society of Japan, Vol.23, No.7, pp. 847-857, 2005 (in Japanese).

Name:
Junichi Mori

Affiliation:
Technological Development Office of Taisho Kensetu Corporation

Address:
2695 Kaneda, Chosei-mura, Chosei-gun, Chiba 299-4332, Japan

Brief Biographical History:
1997- Joined Taisho Kensetu Corporation

Main Works:
• "Development of Quadruped Walking Robot TITAN XI for Steep Slopes –Slope Map Generation and Map Information Application–," Journal of Robotics and Mechatronics, Vol.18, No.3, pp. 318-324, 2006.
• "Development of a Quadruped Walking Robot TITAN XI for Steep Slopes Operation –Conceptual Design and Basic Experiment of Leg Driving Mechanism–," Journal of Robotics Society of Japan, Vol.23, No.7, pp. 847-857, 2005 (in Japanese).